Research Article

Received: 7 January 2022 Revised: 5 April 2022 Accepted article published: 12 May 2022 Published online in Wiley Online Library: 31 May 2022

(wileyonlinelibrary.com) DOI 10.1002/jsfa.12005

# Influence of nanoemulsion/gum ratio on droplet size distribution, rheology and physical stability of nanoemulgels containing inulin and omega-3 fatty acids

**María-Carmen Alfaro-Rodríguez,* P. Prieto, M. C. García, M. J. Martín-Piñero and J. Muñoz**

## Abstract

**Background: New consumer habits are forcing the food industry to develop new and healthy products. In response to this tendency, in this investigation, we obtained nanoemulgels by microfluidization containing inulin fibre and omega-3 fatty acids. First, the influence of the number of microfluidization cycles on the physical properties of the nanoemulsions was studied. Subsequently, an advanced-performance xanthan gum was added to the nanoemulsion in different nanoemulsion/xanthan ratios (1:1, 2:1, 3:1, 4:1, 1:2, and 1:3).**

**Results: Laser diffraction, multiple light scattering, and rheology techniques were used to characterize nanoemulsions and the corresponding nanoemulgels. The nanoemulsion with the lowest Sauter mean diameter (138 nm) and the longest physical stability was obtained after three passes through a microfluidization device at a fixed pressure of 103 421 kPa. Thus, these processing conditions were always used to obtain the nanoemulsion; these were subsequently mixed with a xanthan gum solution to produce nanoemulgels that showed weak gel-like viscoelastic and shear-thinning flow behaviours. A decrease in the nanoemulsion/xanthan ratio (i.e. by an increase in the content of xanthan gum in the nanoemulgel) increased the viscoelastic moduli and the zero shear viscosity values. A rise in the droplet size was observed with aging time, probably due to flocculation. The nanoemulsion/xanthan gum mass ratio of 1:3 yielded the most stable nanoemulgel.**

**Conclusions: This work is a contribution to the development of functional foods. It has been demonstrated that it is possible to obtain a stable nanoemulgel-based food matrix containing fibre and omega-3 fatty acids.**


**Keywords:** nanoemulgel; soybean-and-walnut oil; inulin fibre; xanthan gum; rheology; physical stability

## INTRODUCTION

Currently, new trends in responsible consumption along with greater concern for nutrition and health have driven the development of innovative products containing ingredients that are not only sustainable but that are also healthy and improve health.[1,2] Along these lines, new food products include fibre, antioxidants, vitamins, fatty acids, and so on.

Omega-3 fatty acids have been shown to help fight various diseases, such as Alzheimer's, dementia, dry eye disease, rheumatoid arthritis, cancer, or cardiovascular disease.[3-9] There are three main omega-3 fatty acids: alpha-linoleic acid (ALA), eicosapentaenoic acid, and docosahexaenoic acid. The first of them is an essential fatty acid that is necessary in the diet.[10] In this work, soybean-and-walnut oil was used, which contains 60 g $kg^{-1}$ ALA.

Another essential component of a healthy diet is fibre. A daily intake of about 25 or 30 g is recommended. However, real consumption is much lower than this recommendation. In addition to its properties in the prevention or relief of constipation, dietary fibre also presents other health benefits, such as helping to maintain a healthy weight and to reduce the risk of diabetes, heart disease, and certain types of cancer. There are two types of dietary fibre: insoluble fibre (such as cellulose, lignin, and some hemicelluloses), and soluble fibre (such as gums, mucilages, pectins, and $\beta$-glucans). Inulin Frutafit®, which was used in this work, is a prebiotic-soluble dietary fibre with nutritional and functional properties.

* *Correspondence to: Maria-Carmen Alfaro-Rodriguez, Departamento de Ingeniería Química, Escuela Politécnica Superior, Universidad de Sevilla, C/ Virgen de Africa 7, E41011, Sevilla, Spain, E-mail: alfaro@us.es*

*Departamento de Ingeniería Química, Escuela Politécnica Superior, Universidad de Sevilla, Seville, Spain*

An important concern regarding the incorporation of bioactive ingredients (especially lipophilic compounds) is their bioavailability. For this purpose, a nanoemulsion-based gel (nanoemulgel) constitutes an excellent matrix. The nanoemulgel consists of the addition of a nanoemulsion to a gel-like matrix.[11-13] This formulation makes it possible to combine the advantages of both nanoemulsion and gel. Oil-in-water nanoemulsions are colloidal dispersions of oil droplets with particle sizes ranging from 10 to 500 nm suspended within an aqueous phase.[14-16] The lipophilic ingredient can be included in the oil phase, improving bioaccessibility. This is due to the high interfacial area and small droplet size, which increases the solubility and the dissolution rate through the membranes.[17,18] The addition of hydrogel enhances not only the stability of the nanoemulsion but also the viscosity and texture for a new physical form of presentation. In this work, advanced-performance xanthan gum, produced by the *Xanthomonas campestris* microorganism and manufactured by CP Kelco using an improved fermentation process, was used as a hydrogel matrix. In the past few years, nanoemulgels have been widely studied and applied in pharmaceuticals, and even cosmetics, since their advantages for topical use have been demonstrated. Thus, for example, there are studies of nanoemulgels containing Brazilian red propolis benzophenones to protect the skin from ultraviolet radiation,[19] glimepiride-loaded nanoemulgels for treating diabetes,[20] nanoemulgels containing anti-inflammatory agents,[21] quercetin-loaded nanoemulgels for periodontitis,[22] nanoemulgels containing active food ingredients to treat skin diseases topically,[23] and so on. However, to our knowledge, there are no publications of nanoemulgel-type food products formulated and obtained in the way of those studied in this work.

Energy is necessary to obtain a nanoemulsion. In the food industry, high-pressure homogenization using a microfluidizer makes this possible. This is a device capable of producing nanoemulsions as a result of collisions between particles inside the interaction chamber (y type or z type) and the strong shear, turbulence, and cavitation effects that cause a droplet size reduction.[24,25]

The objective of this work is to develop a nanoemulgel-based food matrix containing omega-3 fatty acids and fibre. For our stated purpose, as a first step, an emulsion containing 250 g $kg^{-1}$ soybean-and-walnut oil and 60 g $kg^{-1}$ inulin Frutafit® was formulated and the influence of the number of recirculation cycles through microfluidizer on the droplet size distribution, rheology, and physical stability was studied. Subsequently, advanced-performance xanthan gum was added to the nanoemulsion in order to obtain the nanoemulgel. The influence of the nanoemulsion/xanthan ratio on the droplet size distribution, rheological properties, and stability of the nanoemulgel was investigated.

This work contributes to meeting the consumer's requirements for a functional food product capable of providing beneficial substances for our health.

## MATERIALS AND METHODS

### Materials

The emulsions were prepared using, as a dispersed phase, soybean-and-walnut oil (La Española, Seville, Spain; 250 g $kg^{-1}$) purchased from a local market. This oil contains 60 g $kg^{-1}$ ALA. Tween 80 (hydrophilic–lipophilic balance value 15; 25 g $kg^{-1}$), supplied by Sigma Aldrich, Spain was used as an emulsifier. Inulin fibre Frutafit® (60 g $kg^{-1}$), kindly provided by Brenntag, was also used. Sodium azide (Panreac, Montcada, Spain) (0.2 g $kg^{-1}$) was added to the samples as a preservative. To complete the emulsion formulation, Milli-Q water was used.

In order to prepare the nanoemulgels, Milli-Q water and high-performance xanthan gum, KELTROL® Advanced Performance, provided by CP Kelco Company (San Diego, CA) were used.

### Preparation of nanoemulgels

In order to obtain the nanoemulsion, the aqueous and dispersed phases were prepared separately. First, the aqueous phase was prepared by adding the appropriate amount of water, sodium azide, and Tween 80. Then, the Frutafit® fibre was slowly added while stirring in an Ultraturrax T50 homogenizer with the S50-G45F dispersion unit at 716 × *g*. Stirring at 179 × *g* was then maintained for 300 s. Subsequently, to obtain the primary emulsion, the oil phase was gradually added at 25 °C. For this purpose, the same homogenizer (Ultraturrax T50) was used for 30 s at 179 × *g* while the oil was added, and then this device was used for an additional 120 s at 716 × *g*. Finally, this primary emulsion was subjected to a high-pressure homogenization procedure using a M-110P microfluidizer (Microfluidics, Spain, USA) at 103 421 kPa.

For the preparation of nanoemulgel[12,26] a stock solution of 10 g $kg^{-1}$ by weight high-performance xanthan gum was first prepared. Then, the nanoemulsion and the gel-like solution of xanthan gum in different ratios (1:1, 2:1, 3:1, 4:1, 1:2 and 1:3) were mixed for 180 s at 8 × *g* using an Ika Visc MR-D1 device (Ika, Staufen, Germany) and a sawtooth-type impeller. The composition of the samples studied is shown in Table 1. The E*X*–*Y* nomenclature will be used to denote the nanoemulgels, with *X*–*Y* being the nanoemulsion/xanthan ratio.

### Sample characterization

Nanoemulsions and nanoemulgels characterization.

### Droplet size distribution

The droplet size distribution of the samples was obtained using a Malvern Mastersizer 2000 laser diffraction device (Malvern Panalytical Ltd, Malvern, UK). Measurements were carried out 24 h after the preparation of the samples. The Sauter diameter $D_{3,2}$ and

**Table 1.** Composition of nanoemulgels studied

| Nanoemulgel | Nanoemulsion/xanthan gum ratio | Xanthan (g $kg^{-1}$) | Fibre (g $kg^{-1}$) | Oil (g $kg^{-1}$) | Omega-3 (g $kg^{-1}$) |
|---|---|---|---|---|---|
| E1–3 | 0.33 | 7.5 | 15 | 63 | 4 |
| E1–2 | 0.50 | 6.7 | 20 | 83 | 5 |
| E1–1 | 1.00 | 5.0 | 30 | 125 | 8 |
| E2–1 | 2.00 | 3.3 | 36 | 150 | 9 |
| E3–1 | 3.00 | 2.5 | 45 | 188 | 11 |
| E4–1 | 4.00 | 2.0 | 48 | 200 | 12 |



  
*Journal of The Science of Food and Agriculture* published by John Wiley & Sons Ltd on behalf of Society of Chemical Industry.

the mean volume diameter $D_{4,3}$ were used to analyse the results.[27] Additionally, the span parameter was employed to quantify the degree of polydispersion. The equations that describe these parameters are as follows:

$$D_{3,2} = \frac{\sum_{i=1}^{N} n_i d_i^3}{\sum_{i=1}^{N} n_i d_i^2} \quad (1)$$

$$D_{4,3} = \frac{\sum_{i=1}^{N} n_i d_i^4}{\sum_{i=1}^{N} n_i d_i^3} \quad (2)$$

where $N$ is the total number of droplets, $d_i$ is the diameter of the droplet, and $n_i$ is the number of droplets having diameter $d_i$.

$$\text{Span} = \frac{(D[v,0.9] - D[v,0.1])}{D[v,0.5]} \quad (3)$$

where $D[v, 0.9]$ and $D[v, 0.1]$ represent the 90th and 10th percentiles and $D[v, 0.5]$ is the median.

Each test was performed three times at room temperature.

### Multiple light scattering

The physical stability of the samples was studied by multiple light scattering using a Turbiscan Lab equipment (Formulaction, Toulouse, France). Backscattering percentage as a function of the length of the vessel containing the sample was determined during the aging time of the samples.

### Rheological characterization

Small-amplitude oscillatory tests and flow curves were performed using a controlled-stress rheometer (Haake Mars, Germany). A coaxial cylinder geometry with treated surface Z20 (inner radius 1 cm, external radius 1.085 cm) was used for the emulsion and a serrated parallel plate geometry of 60 mm in diameter and 1 mm in gap (PP60R) for the emulsion containing xanthan gum. The equilibration time prior to rheological measurements was 300 s, and the temperature was fixed at 20 °C.

To determine the linear viscoelastic range, a stress sweep from 0.1 to 20 Pa was carried out at a fixed frequency of 1 Hz. Then, mechanical spectra were performed from 10 to 0.01 Hz at one shear stress within the linear viscoelastic zone. The flow curves were performed under a controlled stress criterion from 0.1 to 20 Pa.

All measurements were made in duplicate with fresh samples.

## RESULTS AND DISCUSSION

### Nanoemulsions

*Influence of cycles through M110P homogenizer*

Figure 1(A) shows the droplet size distributions of the emulsions as a function of the number of passes or recirculation cycles through microfluidizer. As can be observed in this figure, an increase in the number of cycles shifted the droplet size distribution to lower diameters and the degree of polydispersion decreased. An analysis of the mean size of the droplets and the span (Fig. 1(B)) makes it possible to evaluate in depth the influence of this variable. The low values of the mean Sauter diameter $D_{3,2}$ and the mean volume diameter $D_{4,3}$ obtained after microfluidization should be noted, these being lower than 0.2 μm. From this point of view, these emulsions are nanoemulsions. The mean

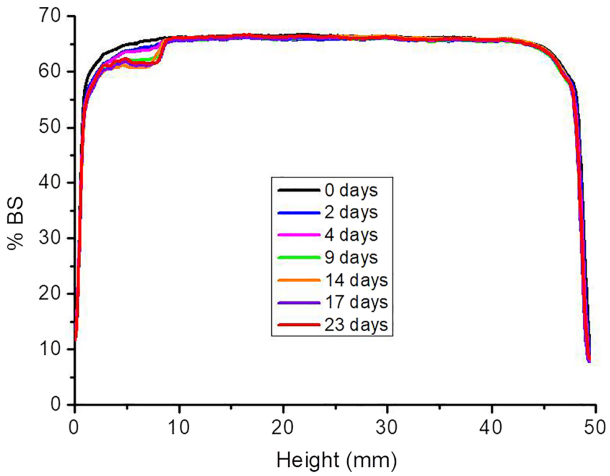


**Figure 2.** Backscattering (BS) as a function of the height of sample and aging time for nanoemulsion. Room temperature.

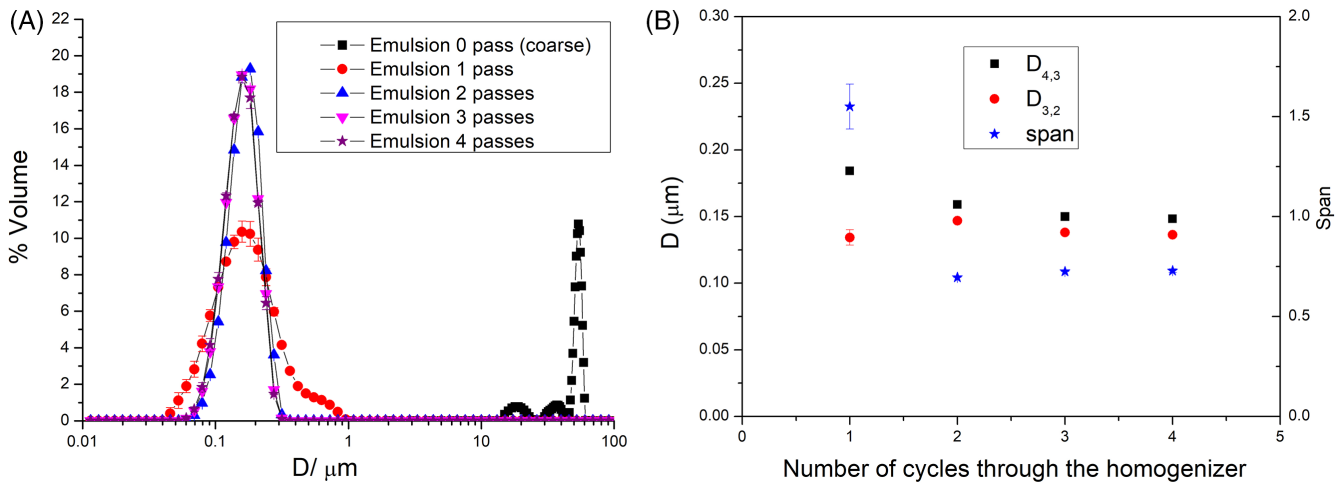


**Figure 1.** (A) Droplet size distributions of emulsion as a function of the microfluidization cycles after production. Pressure: 103 421 kPa. (B) Sauter diameter $D_{3,2}$, mean volume diameter $D_{4,3}$, and span of emulsion as a function of the microfluidization cycles. The standard deviation is also plotted. Room temperature.



*J Sci Food Agric* 2022; **102**: 6397–6403  wileyonlinelibrary.com/jsfa
*Journal of The Science of Food and Agriculture* published by John Wiley & Sons Ltd on behalf of Society of Chemical Industry.

diameters and span tended to decrease with increasing number of cycles, but no significant improvements were observed with more than three passes to justify the application of higher energy. For this reason, three passes were selected as the optimal number of cycles.

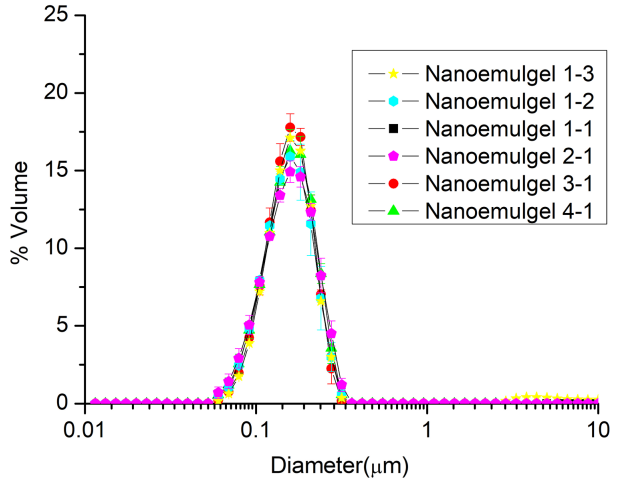


**Figure 3.** Droplet size distribution of nanoemulgels studied. The standard deviation is also plotted. Room temperature.

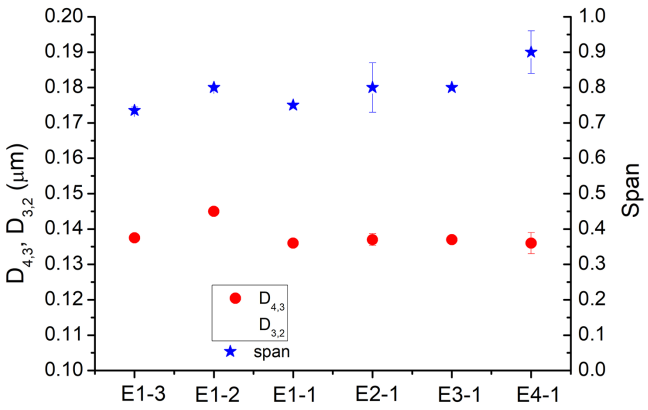


**Figure 4.** Sauter diameter $D_{3,2}$, mean volume diameter $D_{4,3}$, and span of nanoemulgels studied. The standard deviation is also plotted. Room temperature.

*Rheological characterization*

The nanoemulsion did not present measurable elastic component values, and therefore it can be stated that it is essentially viscous and not viscoelastic. Other researchers show similar results for nanoemulsions.[28] The flow behaviour (data not shown) was characterized by presenting a linear variation between the shear stress and the shear rate; that is, the nanoemulsion showed Newtonian behaviour. Its viscosity was determined by applying the Newton model, to which it fitted satisfactorily ($R^2$ = 0.9995), resulting in 8.7 mPa s (almost nine times more viscous than water at 20 °C).

*Physical stability*

The results of multiple light scattering are shown in Fig. 2. A slight decrease in the backscattering (BS) percentage at the bottom was observed, which is related to a creaming destabilization mechanism.

## Nanoemulgels

*Droplet size distribution*

Figure 3 shows the droplet size distributions of the emulgels obtained. Regardless of the nanoemulsion/xanthan ratio, all samples exhibited the same distribution, and this is similar to that presented by the nanoemulsion. This result is consistent with the fact that these samples were obtained from the same emulsion. Additionally, it makes it possible to conclude that the mixing process between nanoemulsion and xanthan gum did not affect the mean droplet size of the nanoemulgel.

An analysis of the mean droplet sizes ($D_{3,2}$ and $D_{4,3}$) corroborated the aforementioned conclusion. As can be seen in Fig. 4, the nanoemulgels showed a mean Sauter diameter value of 140 nm and a mean volumetric mean diameter value of 150 nm. These values were identical to those exhibited by the nanoemulsion after three recirculation cycles. On the other hand, it is worth highlighting the proximity in values of both mean diameters, which means that these systems are very monomodal. See also the low values obtained for the span parameter.

*Rheological characterization*

The storage and loss moduli of the nanoemulsion-based gels *versus* frequency are plotted in Fig. 5(A) and (B) respectively. All samples exhibited storage modulus values much higher than the loss modulus values in the whole frequency range studied. No crossover is observed. Furthermore, they presented a low

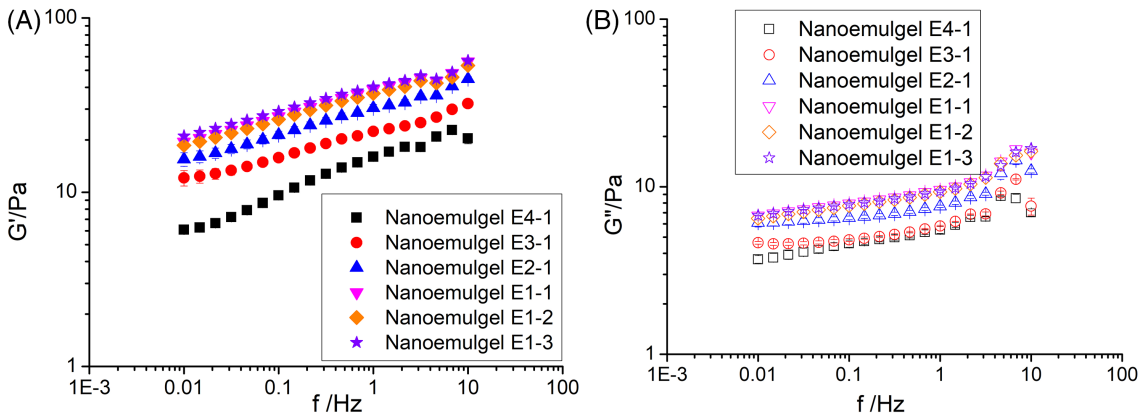


**Figure 5.** Influence of frequency on (A) storage modulus $G'$ and (B) loss modulus $G''$ of nanoemulgels studied. The standard deviation is also plotted. $T$ = 20 °C.



  
*Journal of The Science of Food and Agriculture* published by John Wiley & Sons Ltd on behalf of Society of Chemical Industry.

frequency dependence, as demonstrated by the slight slope exhibited by the curves. These mechanical spectra are typical of strong gel-like structures. However, the fact that the difference between the storage modulus and the loss modulus is less than one order of magnitude indicated the occurrence of a weak gel-like structure.[29,30] Viscoelastic moduli increased with increasing concentration of xanthan gum in the nanoemulgel, probably because of the existence of a higher polymer entanglement. In addition, a trend to a reduction in the slope of $G'$ was observed (Fig. 5(A)), indicating a higher solid-like behaviour of the system.[31] Other researchers[32,33] also found similar results, but in nanoemulsions of fennel oil (10 g kg$^{-1}$) or nanoemulsions of rosemary oil (200 g kg$^{-1}$) containing advanced-performance xanthan gum that was added as powder after emulsification. It should be noted that in our work the nanoemulsion is added to a gel-like solution of advanced-performance xanthan gum. We found that below 5 g kg$^{-1}$ of gum, an increase in xanthan content in the nanoemulsion-based gel provoked a significant increase in both viscoelastic moduli (compare the values of $G'$ and $G''$ in the samples E4–1, E3–1, E2–1, and E1–1), whereas nanoemulgels E1–1, E1–2, and E1–3 containing a xanthan gum concentration above 5 g kg$^{-1}$ exhibited a smaller difference between the values of $G'$. In this study, E4–1, with the lowest xanthan gum content (2 g kg$^{-1}$), was the nanoemulgel with the lowest viscoelastic moduli values, and E1–3 had the highest values.

The flow behaviour of the nanoemulgels was shear thinning (Fig. 6), which was due to the progressive disruption of the structure of the nanoemulgel under the influence of applied shear stress.[34] Samples containing higher xanthan gum content had a similar flow behaviour, with zero-shear viscosity $\eta_0$ close to 3000 Pa s. However, $\eta_0$ values of the E2–1, E3–1, and E4–1 nanoemulgels decreased with the increase in the nanoemulsion/xanthan ratio in the sample.

The flow curves fitted well ($R^2 = 0.99$) to the Cross model:[35]

$$\eta_a = \eta_\infty + \frac{\eta_0 - \eta_\infty}{1 + (\dot{\gamma}/\dot{\gamma}_c)^{1-n}} \quad (4)$$

where $\eta_a$ (Pa s) is the apparent viscosity, $\dot{\gamma}$ (s$^{-1}$) the shear rate, $\eta_0$ (Pa s) is the zero-shear rate viscosity, $\eta_\infty$ (Pa s) is the infinite shear rate viscosity, $\dot{\gamma}_c$ (s$^{-1}$) is related to the critical shear rate for the onset of the shear-thinning response, and $(1 - n)$ is a dimensionless parameter related to the slope of the power-law region, with $n$ being the so-called 'flow index'. It should be noted that since the high-shear Newtonian zone was never achieved in this study, Eqn (4) was simplified, neglecting $\eta_\infty$ since $\eta_\infty \ll \eta_0$.

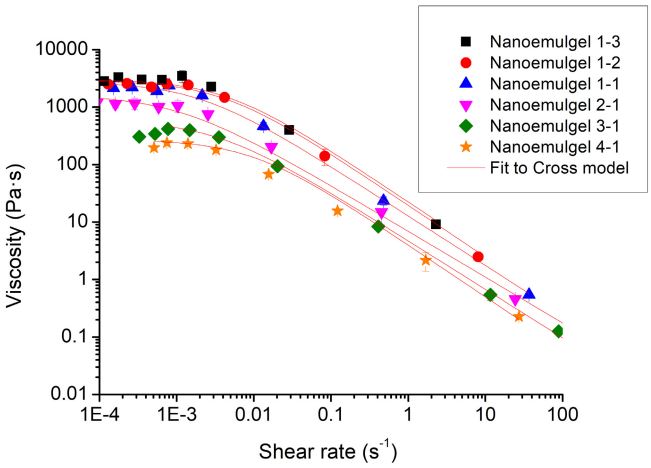


**Figure 6.** Viscosity *versus* shear rate as a function of nanoemulsion/hydrogel ratio studied. Additionally, the fit to the Cross model is plotted. $T = 20$ °C.

The fitting parameters are shown in Table 2. The zero-shear viscosity values obtained corroborated what was visually observed; that is, its value increased when the amount of xanthan gum in nanoemulgel increased (from 2 to 5 g kg$^{-1}$ of xanthan gum), although it remained practically constant for systems with higher gum content (E1–3, E1–2, and E1–1 samples). The critical shear rate and the flow index values were not sensitive to the nanoemulsion/xanthan ratio, and their values were not significantly different for all nanoemulsion-based gels studied, showing similar degrees of shear thinning.

Multiple light scattering results for E4–1 and E1–3 are shown in Fig. 7(A) and (B) respectively by way of an example. A decrease in the percentage of backscattering can be observed throughout the entire measuring cell. This decrease was most important during the first hours or days of aging, depending on the sample, but it was subsequently less important. According to multiple light scattering theory,[36] the observed changes indicated the occurrence of an increase in droplet size without differentiating between flocculation or coalescence. It is hypothesized that these nanoemulgels are flocculated; in any case, whether it is coalescence or flocculation that subsequently leads to coalescence, it is a very slow process, since the samples appeared visually stable at 4 months of aging time.

The stability of nanoemulgels has been quantified by the following equation:

$$\%\Delta BS = \frac{BS_{t=0} - BS_{t=15\ days}}{BS_{t=0}} \times 100 \quad (5)$$

where $BS_{t=0}$ is the mean value of the percentage of backscattering at the initial time (time 0) and $BS_{t=15\ days}$ is the mean value of the percentage of backscattering at 15 days of aging. According to Eqn (5), the higher the percentage $\Delta BS$ value the more unstable the sample is. The results are shown in Fig. 7(C). It can be observed that the instability of the sample increased with increasing nanoemulsion/xanthan gum ratio in the nanoemulgel; namely, with decreasing xanthan gum concentration. Thus, the most stable nanoemulsion-based gel was E1–3, and the most unstable nanoemulgel was E4–1.

The results obtained from rheology and multiple light scattering were consistent. Therefore, it can be stated that a higher concentration of xanthan gum in the nanoemulgel increased the viscosity and the viscoelastic moduli ($G'$ and $G''$), and this fact hindered the movement of droplets. As a consequence, the degree of

**Table 2.** Fitting parameters to the Cross model

| Nanoemulgel | $\eta_0$ (Pa s) | $\dot{\gamma}_c$ (s$^{-1}$) | $n$ |
|---|---|---|---|
| E1–3 | 3029.2 ± 96.5 | 0.004 ± 0.000 | 0.10 ± 0.00 |
| E1–2 | 2888.0 ± 110.64 | 0.004 ± 0.000 | 0.10 ± 0.00 |
| E1–1 | 2746.8 ± 149.2 | 0.002 ± 0.000 | 0.14 ± 0.07 |
| E2–1 | 1638.5 ± 572.8 | 0.001 ± 0.000 | 0.20 ± 0.02 |
| E3–1 | 602.2 ± 82.4 | 0.003 ± 0.000 | 0.16 ± 0.04 |
| E4–1 | 271.7 ± 16.4 | 0.001 ± 0.000 | 0.10 ± 0.05 |



  
*Journal of The Science of Food and Agriculture* published by John Wiley & Sons Ltd on behalf of Society of Chemical Industry.

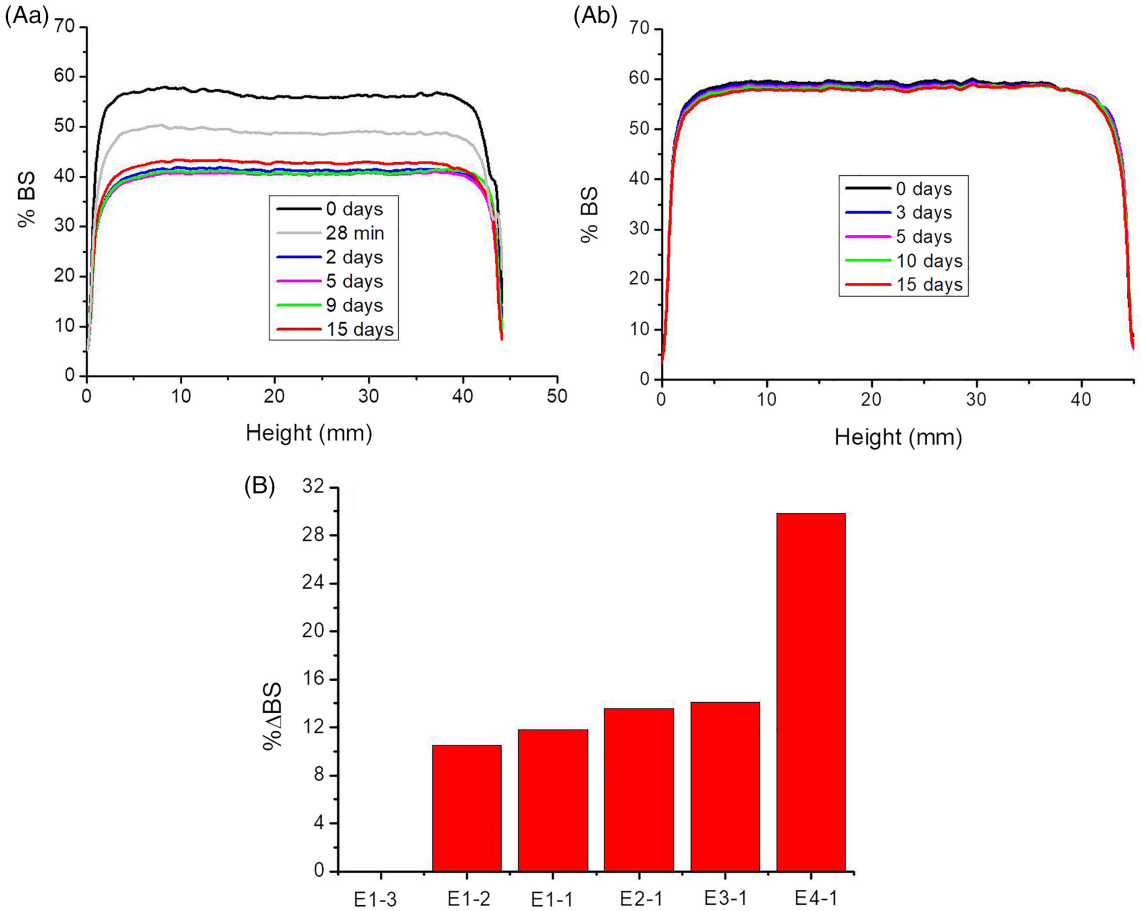


**Figure 7.** (A) Backscattering percentage as a function of the sample height and aging time: (A) E4–1; (B) E1–3. (B) Percentage destabilization of nanoemulgels at 15 days of aging. Room temperature.

flocculation with aging time was lower. The lower oil concentration, and therefore the lower fraction by volume of droplets, also contributed to this lower degree of flocculation. For this reason, the most stable nanoemulgel was E1–3, whereas E4–1 was the most unstable.

## CONCLUSIONS

We have demonstrated that it is possible to obtain soybean-and-walnut oil nanoemulsions in water, formulated with inulin fibre using the microfluidization technique. First, the number of microfluidization cycles to obtain low droplet diameter and high physical stability was optimized. The results indicated that three cycles was the optimal number. The nanoemulsion obtained exhibited a Sauter mean diameter of 138 nm and a Newtonian flow behaviour with a viscosity value of 8.7 mPa s. In addition, the nanoemulsion lacks a measurable linear viscoelastic region. Next, stock xanthan gum solution of 1 g $kg^{-1}$ was added in different ratios to the nanoemulsion to obtain the nanoemulgels and to improve the stability and rheological properties of the nanoemulsion. The method of preparation used to obtain these nanoemulgels did not have any influence on the droplet size distribution. Hence, all emulgels presented the same distribution as the starting nanoemulsion. Regardless of the nanoemulsion/xanthan ratio, all of the nanoemulgels studied showed weak gel-like viscoelastic behaviour. The amount of xanthan gum controlled the rheology of the nanoemulgel. Thus, a decrease in the emulsion/xanthan ratio, which means a higher concentration of xanthan gum, caused a larger extension of the linear viscoelastic region, higher values of viscoelastic moduli ($G'$ and $G''$), and higher values of zero-shear viscosity. The aging time caused an increase in droplet sizes in all nanoemulsion-based gels, probably due to a flocculation process. This fact was less important when the emulsion/xanthan ratio decreased, that is, with an increase in the percentage of xanthan gum in the formulation. The nanoemulgel obtained at the 1:3 nanoemulsion/xanthan ratio (E1–3) turned out to be the most stable and additionally exhibited the highest viscoelastic moduli and zero-shear viscosity values of all the formulations studied.

This work contributes to the development of functional foods. This product satisfies today's consumers, who are more aware of the need for a healthy diet.

## ACKNOWLEDGEMENTS

We are grateful to the Universidad de Sevilla (Spain) (VI Plan Propio de Investigación, project PP2019-13291).

## REFERENCES

1 Asioli D, Aschemann-Witzel J, Caputo V, Vecchio R, Annunziata A and Næs T, Making sense of the 'clean label' trends: a review of consumer food choice behaviour and discussion of industry implications. *Food Res Int* **99**:58–71 (2017).



  

2 Aschemann-witzel J and Peschel AO, Consumer perception of plant-based proteins: the value of source transparency for alternative protein ingredients. *Food Hydrocoll* **96**:20–28 (2019).
3 MacLean CH, Issa AM, Mojica WA, Newberry SJ, Morton SC, Shekelle PG *et al*., *Effects of Omega-3 Fatty Acids on Cognitive Function with Aging, Dementia, and Neurological Diseases*. Agency for Healthcare Research and Quality, Rockville, MD (2005).
4 Simopoulos AP, The importance of the omega-6/omega-3 fatty acid ratio in cardiovascular disease and other chronic diseases. *Exp Biol Med* **233**:674–688 (2008).
5 Liu A and Ji J, Omega-3 essential fatty acids therapy for dry eye syndrome: a meta-analysis of randomized controlled studies. *Med Sci Monit* **20**:1583–1589 (2014).
6 Kakoti BB, Hernandez-Ontiveros DG, Kataki MS, Shah K, Pathak Y and Panguluri SK, Resveratrol and omega-3 fatty acid: its implications in cardiovascular diseases. *Front Cardiovasc Med* **2**:38 (2015).
7 Akbar U, Yang M, Kurian D and Mohan C, Omega-3 fatty acids in rheumatic diseases: a critical review. *J Clin Rheumatol* **23**:330–339 (2017).
8 Freitas RD and Campos MM, Protective effects of omega-3 fatty acids in cancer-related complications. *Nutrients* **11**:945 (2019).
9 Marti A and Fortique F, Omega-3 fatty acids and cognitive decline: a systematic review. *Nutr Hosp* **36**:939–949 (2019).
10 Guiotto EN, Ixtaina VY, Nolasco SM and Tomás MC, Effect of storage conditions and antioxidants on the oxidative stability of sunflower–chia oil blends. *J Am Oil Chem Soc* **91**:767–776 (2014).
11 Eid AM, El-Enshasy HA, Aziz R and Elmarzugi NA, Preparation, characterization and anti-inflammatory activity of *Swietenia macrophylla* nanoemulgel. *J Nanomed Nanotechnol* **5**:1–10 (2014).
12 Anand K, Ray S, Rahman M, Shaharyar A, Bhowmik R, Bera R *et al*., Nano-emulgel: emerging as a smarter topical lipidic emulsion-based nanocarrier for skin healthcare applications. *Recent Pat Antiinfect Drug Discov* **14**:16–35 (2019).
13 Sungpud C, Panpipat W, Chaijan M and Sae YA, Techno-biofunctionality of mangostin extract-loaded virgin coconut oil nanoemulsion and nanoemulgel. *PLoS One* **15**:e0227979 (2020).
14 Otoni CG, Avena-Bustillos RJ, Olsen CW, Bilbao-Sáinz C and McHugh TH, Mechanical and water barrier properties of isolated soy protein composite edible films as affected by carvacrol and cinnamaldehyde micro and nanoemulsions. *Food Hydrocolloids* **57**:72–79 (2016).
15 Rao J and McClements DJ, Food-grade microemulsions, nanoemulsions and emulsions: fabrication from sucrose monopalmitate & lemon oil. *Food Hydrocolloids* **25**:1413–1423 (2011).
16 Weiss J, Decker EA, McClements DJ, Kristbergsson K, Helgason T and Awad T, Solid lipid nanoparticles as delivery systems for bioactive food components. *Food Biophys* **3**:146–154 (2008).
17 Anand P, Kunnumakkara AB, Newman RA and Aggarwal BB, Bioavailability of curcumin: problems and promises reviews bioavailability of curcumin: problems and promises. *Mol Pharm* **4**:807–818 (2007).
18 Araiza-Calahorra A, Akhtar M and Sarkar A, Recent advances in emulsion-based delivery approaches for curcumin: from encapsulation to bioaccessibility. *Trends Food Sci Technol* **71**:155–169 (2018).
19 Correa L, de Carvalho Meirelles G, Balestrin L, Oliveira de Souza P, Fonseca Moreira JC, Silvestri Schuh R, et al. *In vitro* protective effect of topical nanoemulgels containing Brazilian red propolis benzophenones against UV-induced skin damage, *Photochem Photobiol Sci* **19**(10): 1460–1469 (2020).
20 Razzaq FA, Asif M, Asghar S, Iqbal MS, Khan IU, Khan SUD *et al*., Glimepiride-loaded nanoemulgel; development, *in vitro* characterization, *ex vivo* permeation and *in vivo* antidiabetic evaluation. *Cell* **10**:2404 (2021).
21 Eid AM, El-Enshasy HA, Aziz R and Elmarzugi NA, Preparation, characterization and anti-inflammatory activity of *Sweetenia macrophylla* nanoemulgel. *J Nanomed Nanotechnol* **5**:1000190 (2014).
22 Aithal GC, Nayak UY, Mehta C, Narayan R, Gopalkrishna P, Pandiyan S *et al*., Localized *in situ* nanoemulgel drug delivery system of quercetin for periodontitis: development and computational simulations. *Molecules* **23**:1363 (2018).
23 Chang WC, Hu YT, Huang Q, Hsieh SC and Ting Y, Development of a topical applied functional food formulation: adlay bran oil nanoemulgel. *LWT* **117**:108619 (2020).
24 Microfluidics, *Microfluidizer Processor User Guide*. [Online] (2014). https://www.alfatest.it/keyportal/uploads/2017-microfluidics-chamber-user-guide.pdf [3 November 2022].
25 Ozturk OK and Turasan H, Latest developments in the applications of microfluidization to modify the structure of macromolecules leading to improved physicochemical and functional properties. *Crit Rev Food Sci Nutr* (2021). https://doi.org/10.1080/10408398.2021.1875981.
26 Sengupta P and Chatterjee B, Potential and future scope of nanoemulgel formulation for topical delivery of lipophilic drugs. *Int J Pharm* **526**:353–365 (2017).
27 McClements DJ ed, *Food Emulsions: Principles, Practices and Techniques*, 2nd edn. CRC Press, Boca Raton, FL, USA (2005).
28 Martin-Piñero MJ, Muñoz J and Alfaro-Rodriguez MC, Improvement of the rheological properties of rosemary oil nanoemulsions prepared by microfluidization and vacuum evaporation. *J Ind Eng Chem* **91**:340–346 (2020).
29 Martín-Piñero MJ, García MC, Muñoz J and Alfaro-Rodríguez MC, Influence of the welan gum biopolymer concentration on the rheological properties, droplet size distribution and physical stability of thyme oil/W emulsions. *Int J Biol Macromol* **133**:270–277 (2019).
30 Wyatt NB and Liberatore MW, Rheology and viscosity scaling of the polyelectrolyte xanthan gum. *J Appl Polym Sci* **114**:4076–4084 (2009).
31 Song K-W, Kim Y-S and Chang G-S, Rheology of concentrated xanthan gum solutions: steady shear flow behaviour. *Fibers Polym* **7**:129–138 (2006).
32 Llinares R, Ramírez P, Carmona JA, Trujillo-Cayado LA and Muñoz J, Assessment of fennel oil microfluidized nanoemulsions stabilization by advanced performance xanthan gum. *Foods* **10**:693 (2021).
33 Martin-Piñero MJ, García MC, Santos J, Alfaro-Rodriguez MC and Muñoz J, Characterization of novel nanoemulsions, with improved properties, based on rosemary essential oil and biopolymers. *J Sci Food Agric* **100**:3886–3894 (2020).
34 Behera B, Biswal D, Uvanesh K, Srivastava AK, Bhattacharya MK, Paramanik K *et al*., Modulating the properties of sunflower oil based novel emulgels using castor oil fatty acid ester: prospects for topical antimicrobial drug delivery. *Colloids Surf B* **128**:155–164 (2015).
35 Cross MM, Rheology of non-Newtonian fluids: a new flow equation for pseudoplastic systems. *J Colloid Sci* **20**:417–437 (1965).
36 Mengual O, Meunier G, Cayre I, Puech K and Snabre P, Characterisation of instability of concentrated dispersions by a new optical analyser: the TURBISCAN MA 1000. *Colloids Surf A* **152**:111–123 (1999).




  
*Journal of The Science of Food and Agriculture* published by John Wiley & Sons Ltd on behalf of Society of Chemical Industry.